Himawari-8 Land Surface Temperature data capture frost across the Australian grain belt

Ha Thanh Nguyen[1], Roger Lawes[2], Randall Donohue[1], Quanxi Shao[3] and David Deery[1]
[1]Commonwealth Scientific and Industrial Research Organization, Black Mountain, ACT 2601, ngu197@csiro.au
[2] Commonwealth Scientific and Industrial Research Organization, Floreat, WA, 6010
[3] Commonwealth Scientific and Industrial Research Organization, Kensington, WA, 6151

Abstract
Australia is facing an increase in cold extremes associated with damaging spring frost events. Frost damage in crops has been defined using screen air temperatures from nearby weather stations, which may not represent the crop temperature below the screen height or the specific place of frost occurrence. Remotely sensed Land Surface Temperature (LST) approximates skin temperature over crops and can overcome the afore-mentioned spatial limitation. However, LST retrieval, and frost detection from LST, is challenging as current cloud screening algorithms have limited success with night-time, local cloud occurrences. We designed a set of statistical change-point detection methods for the integrated LST time series and air temperature data that could be used to distinguish clear (cloud-free) conditions, which are conducive to frosts, from cloudy conditions, so that true LST values can be reliably acquired at night. The statistical feature of choice, which is a moving hourly variance, reduced the RMSE in the original LST data by a factor of 2. Henceforth, clear/cloud night assessments were generated dynamically to adapt to observed changes in background and/or climatic conditions, facilitating a robust detection and analysis technique for agricultural frosts.

Introduction

Frost incurs more serious economic losses than any other climate-related risks for countries with temperate to arid climates. In Australia, economic losses from radiation frost damage especially between heading and grain-filling period (late winter to spring) have been estimated at up to $360 million per year. Radiation frosts typically occur when energy loss by longwave radiation is greater from the upper layers of the crop compared with that occurring at or near the soil surface. The impact of radiation frost may also increase in the future due to drier atmospheric conditions and clear nights, which results in an increase in night-time radiative energy loss combined with rapid development of crops and earlier flowering under warmer daytime temperatures.

The potential for frost damage in crops has been defined as a situation where air temperature (T_a) declines to ≤0°C at canopy height, which is approximately equivalent to 2°C T_a in a Stevenson screen at 1200-1500mm above ground level. Remotely sensed Land Surface Temperature (LST), retrieved from spaceborne thermal infra-red (TIR) sensors, provides a more direct approximation of skin temperature over crops but is only available under clear sky observations. Existing cloud masking algorithms were designed for polar orbiting sensors, with lower temporal resolution than the geostationary LST. Existing cloud masking techniques from other satellites are unsuitable.

In this study, we created an analytical process to predict clear calm temperature patterns over dryland crops using a combination of geostationary LST, proximally sensed air temperature, and statistical techniques that leveraged the high temporal information content of the former. We extracted features from LST profiles during several spring frosts events in late 2023 at the Boorowa Agricultural Research Station (34° 28' 48" S, 148° 41' 24" E). Two questions were investigated: 1) do temperature patterns during clear calm nights when frost happens statistically differ from those during cloudy nights and 2) what is the best statistical feature that can operationally characterize these clear calm nights?

Methods

Site description and event description
At the Boorowa Agricultural Research Station (34° 28' 48" S, 148° 41' 24" E), several frosts events naturally occurred on October 17, 25 and November 1, 2023 (personal communication. During the most severe frost (October 25), various air temperature sensors recorded minimum night-time air temperatures between -6.5° and -1.5°C between 2.20am and 4.30am local time (17.42 – 19.23UTC).

Himawari-8 Land Surface Temperature (LST)
The Advanced Himawari Imager (AHI) onboard Himawari-8 contains six visible (VIS) and near infrared (NIR) bands centered at 0.47, 0.51, 0.64, 0.86, 1.61, and 2.25 μm, as well as ten infrared (IR) bands centered at 3.9, 6.2, 6.9, 7.3, 8.6, 9.6, 10.4, 11.2, 12.4 and 13.3 μm. The split-window algorithm was adapted for Himawari-8, which generated LST at 2 km and 10 minutes resolutions.

Construction and deconstruction of a clear-night radiative cooling pattern
To create a training set of temperature patterns, we extracted the Himawari-8 land surface temperatures and other relevant micrometeorological measurements (outgoing longwave radiation and air temperatures) on the reported event. We tested several statistical descriptors that were designed to leverage the short-term variations in LST to maximize the filtering power for identifying pixels that did not exhibit the locally expected diurnal variations.

Results

We compared the patterns and moving statistics of LST during frost with coincidental air temperatures and long wave radiations sensors at BARS during October 25-26, 2023.

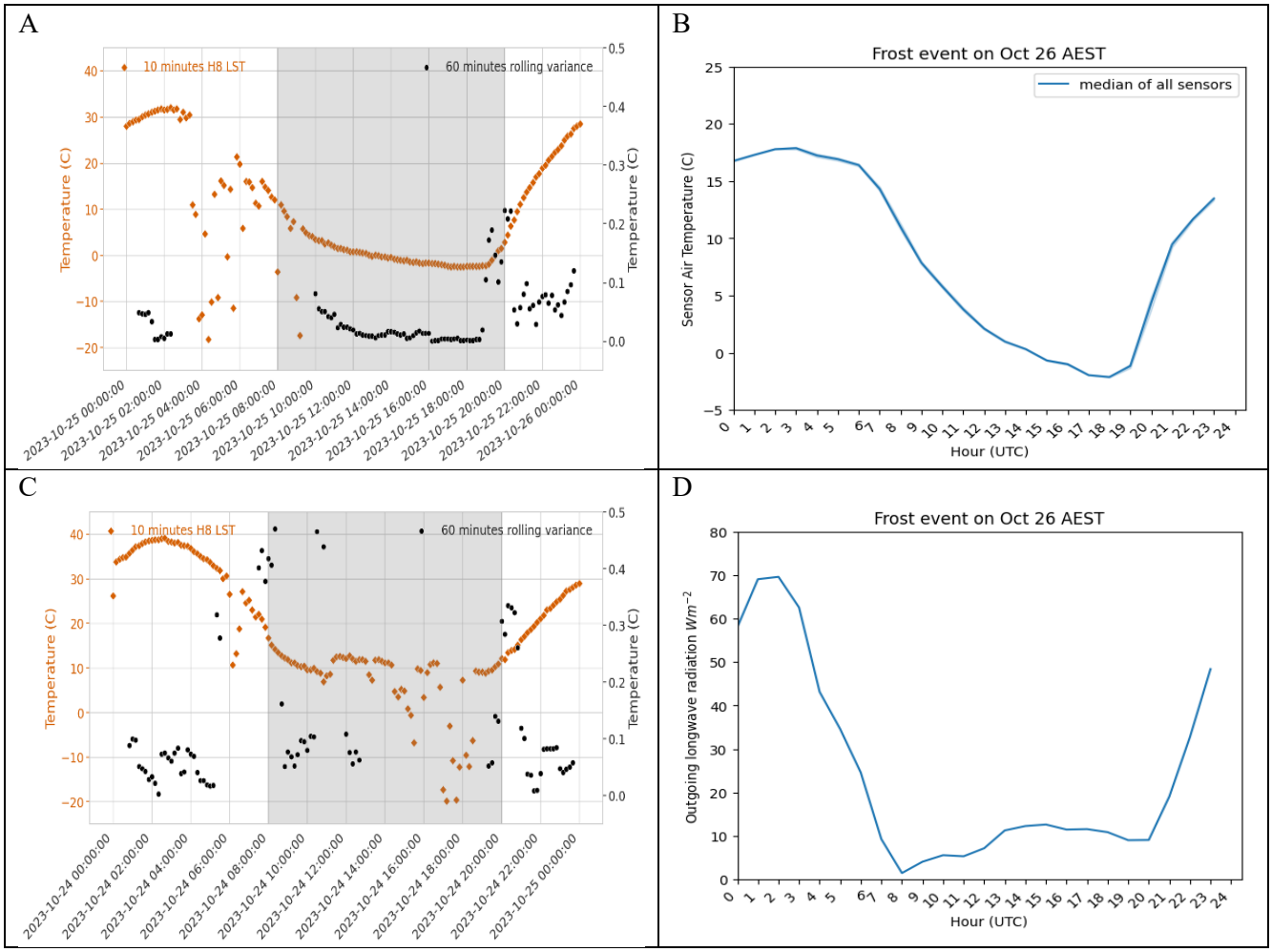

Figure 1: Statistical features of a frost event. Note: The extremely large 60 minutes rolling variance is not plotted if it is out of the plotting range.

At the Boorowa Agricultural Research Station, various air temperature sensors recorded minimum night-time air temperatures between -6.5° and -1.5°C between 2.20am and 4.30am local time (17.42 – 19.23UTC) (Figure 1B). Since the on-site incoming long-wave radiometer failed, we assumed that the outgoing longwave radiation dominated the nocturnal energy budget and closely represented the pattern in surface temperature. Retrieved outgoing long wave radiation (Figure 1D) during the frost event on October 26, 2023 showed that after the initial rapid drop in temperature, the cooling rates decreased steadily until the overnight minimum was achieved just before sunrise. Two minima in outgoing long wave radiation occurred at local sunset (8:00 UTC) and then just before sunrise (20:00 UTC). The second minimum in outgoing longwave radiation coincided with overnight air and land surface temperatures (Figure 1A-B).

We also compared the patterns and moving statistics of LST during frost (25/10/2023 UTC) with that during no-frost conditions on an adjacent night (24/10/2023 UTC) (Figure 1C). LST data on a frost night had few spurious values (Figure 1A) , whereas those on a non-frost night displayed extensive periods of noise (Figure 1D) between sunset and pre-sunrise minimum. During the frost event, the moving variances of LST ranged from 0 to 0.1 for most of the night. Within 1 hour before and after sunrise, or between 7 and 8pm UTC, the variance in LST rose to just under 0.25. In contrast, on a frost-free night, the moving variances of LST regularly exceeded 0.3.

The frost and frost-free time series of LST illustrated that if and when nocturnal clouds occurred, there existed a time when the moving hourly variance in LST exceeded 0.3. When there was no nocturnal cloud, the moving hourly variances in LST stayed below 0.3. Effectively, we have extracted the statistical features of the weather pattern that leads to frost.

We then computed the moving hourly variance on LST data over BARS for previous years in the archive (2016-2022) and applied a constraint of $0.3K^2\ h^{-1}$. This temporal threshold more than halved the RMSE error from 7.86K (Fig 2A) to 3.37K (Fig 2B). The low R^2 value (0.38) was due to remaining low values and noise.

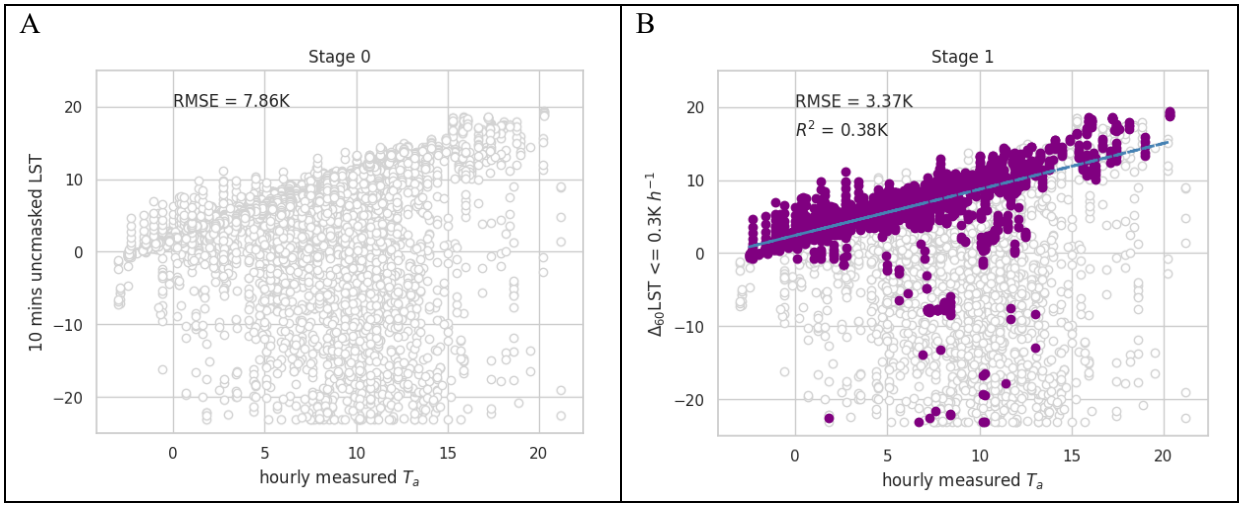

Figure 2: LST to T_a relationship at BARS during August-October 2020 before (A) and after (B) imposing a threshold on moving hourly variance

Conclusion

Cloud cover directly affects the quality and the accuracy of Land Surface Temperature retrieval from Thermal Infrared. Most cloud masking methods were designed for polar-orbiting sensors and did not directly apply to geostationary sensors. Whereas LST gap reconstruction methods were not feasible for use at night-time. In this paper, we described the distinct radiative cooling pattern under clear sky condition and exploited the temporal structure and statistics only possible with geostationary LST. The statistical feature of choice, which is a moving hourly variance, reduced RMSE in the original LST data by a factor of 2. Given the association between calm clear nights and radiation frost, one direct application of cloud masked LST time series was suitable for frost risk mapping.

References

Nuttall, J.G.; Perry, E.M.; Delahunty, A.J.; O'Leary, G.J.; Barlow, K.M.;Wallace, A.J. Frost response in wheat and early detection using proximal sensors. J. Agron. Crop Sci. 2019, 205, 220–234.

Snyder, R. L. and de Melo-Abreu, J. P.: "Frost Protection: fundamentals, practice and economics" Volume 1., Food and Agriculture Organization of the United Nations, FAO, 2005.

Marcellos, H., & Single, W. V. (1984). Frost injury in wheat ears after ear emergence. Functional Plant Biology, 11(2), 7-15.